Synthesis and Characterization of Indole-Based Azomethine Compounds and Investigation of Their Dielectric Properties in Polyvinyl Alcohol Films

Maryam Ahmed Rostom Abdulwahhab H. Majeed*

Department of Chemistry- College of Science- University of Diyala

maryamahmed٨٨٢٥@gmail.com abdulwahhab@uodiyala.edu.iq

Abstract:

The following study reports on the synthesis of a series of organo-Schiff bases (M١–M٥) through condensation reactions between indole-٣-carboxaldehyde and various aromatic and heterocyclic amines such as ٤-aminoacetophenone, ٢-aminobenzothiazole, ٢-aminothiazole, ٢-aminopyridine, and ٥-amino-١,٣,٤-thiadiazole-٢-thiol. The synthesized compounds were characterized by FTIR and ^{1}H-NMR techniques for confirmation of the proposed structures. Since these compounds do not form stable films in the solid state, they were incorporated into a polyvinyl alcohol matrix, and composite films were prepared using the solution casting technique to study their electrical properties. The measurements revealed that all composite films are characterized by a decrease in the true dielectric constant (ε′) with increasing frequency, whereas both imaginary permittivity (ε″) and alternating current conductivity (σ(ac)) increase with increasing frequency. The results also indicated that the electrical properties depend on the molecular structure of the Schiff base compounds. Among them, the film containing compound M٤ showed the highest values of dielectric permittivity and conductivity, while the M١ and M٢ films showed the lowest values of dielectric loss and conductivity.

Keywords: Indole-٣-carboxaldehyde, Schiff base, Dielectric Properties, Poly (Vinyl Alcohol).

تحضير وتشخيص مركبات الأزوميثين القائمة على الإندول ودراسة خصائصها العازلية الكهربائية في أغشية بولي (فينايل الكحول)

مريم أحمد رستم عبد الوهاب حميد مجيد

قسم الكيمياء– كلية العلوم–جامعة ديالى

الخلاصة:

تتناول هذه الدراسة تخليق سلسلة من قواعد شيف العضوية (M١–M٥) من خلال تفاعلات التكثيف بين إندول–٣–كربوكسالدهيد ومجموعة متنوعة من الأمينات العطرية وغير المتجانسة، مثل ٤–أمينوأسيتوفينون، و٢–أمينوبنزوثيازول، و٢–أمينوثيازول، و٢–أمينوبيريدين، و٥–أمينو–١،٣،٤–ثياديازول–٢–ثيول. تم توصيف المركبات المُصنّعة باستخدام تقنيات FTIR و^{1}H–NMR لتأكيد البنى المقترحة. ولأن هذه المركبات لا تُشكّل أغشية مستقرة في الحالة الصلبة، فقد تم دمجها في مصفوفة من كحول البولي فينيل، وتم تحضير أغشية مركبة باستخدام تقنية صب المحلول لدراسة خصائصها الكهربائية. وكشفت القياسات أن جميع الأغشية المركبة تتميز بانخفاض في ثابت العزل الكهربائي الحقيقي (ε′) مع زيادة التردد، بينما تزداد كل من السماحية التخيلية (ε″) وموصلية التيار المتردد (σ(ac)) مع زيادة التردد. كما أشارت النتائج إلى أن الخصائص الكهربائية تعتمد بشكل أساسي على البنية الجزيئية لمركبات قاعدة شيف. ومن بينها، أظهر الغشاء الذي يحتوي على المركب M٤ أعلى قيم لثابت العزل الكهربائي والموصلية، بينما أظهر الغشاءان M١ و M٢ أدنى قيم لفقد العزل الكهربائي والموصلية.

الكلمات المفتاحية : اندول–٣–كربوبوكسالدهيد ، قاعدة شيف ، الخصائص العازلة ، بولي (فينيل الكحول) .

* Corresponding author : Abdulwahhab H. Majeed .

١. Introduction

Schiff bases in organic chemistry are among the most important chemical classes and have been widely used since their discovery. The presence of the imine group (-N=CH-) is what distinguishes Schiff bases due to the presence of the double bond, which gives them unique structural and reactive properties. The other names by which these compounds are known are azomethines or imines, which are usually formed by the reaction of carbonyl compounds (aldehydes or ketones) with primary [١, ٢]. The significant diversity of amine and carbonyl compounds used in condensation reactions (Schiff bases) allows for the design of various azomethine compounds with controllable structural and coordination properties, according to their fields or targeted applications. This distinction opens up an unlimited number of possibilities for synthesizing these different chemical compounds, creating a wide range of applications used and permitted within this scope [٣, ٤]. Due to their numerous properties, Schiff bases are of particular importance, including their ease of synthesis, flexible coordination, thermal stability, and ability to form new structures with diverse biological activities [٥, ٦]. Several Schiff base derivatives possess antioxidant properties, as indicated by numerous studies [٧], their effectiveness in pain relief [٨], anti-cancer activities [٩], antifungal properties [١٠], and also their efficacy against leishmaniasis [١١]. In addition to biological applications, Schiff base compounds are used in many other applications, such as environmental, industrial, and energy applications. They are widely used in removing pollutants from the environment, such as heavy metals[١٢] or dyes [١٣] from water, oil. They are also used as sensors to detect certain pollutants in the air[١٤, ١٥]. Some Schiff bases are used to reduce corrosion of pipes, plates, and similar materials[١٦]. Furthermore, they are used in energy storage devices, sensors, electrical insulation applications, and in the preparation of polymer films for this purpose [١٧-١٩].

Electrical dielectric and electrical conductivity are fundamental physical properties of organic compounds, governing their behavior under electric field conditions and determining their suitability for electronic and optical applications. Most organic compounds are weak dielectrics or semiconductors due to the covalent nature of their bonds and the scarcity of free charge carriers[٢٠]. However, these properties are directly influenced by the molecular structure of the compound. Key factors affecting dielectric properties include molecular polarity, the degree of electron conjugation (π-conjugation), the type of aromatic or heterocyclic rings, the nature of the functional groups, and the degree of structural asymmetry[٢١]. Increased polarity and polarizability lead to a higher true dielectric constant, ε', at low frequencies. Schiff's bases are of particular interest in this area because they contain an azimine bond (-C=N-), which acts as an active center for polarization and charge transfer. The combination of this bond with nitrogen- or sulfur-rich heterocyclic rings such as thiazole, pyridine, and indole enhances directional polarization and increases the dielectric loss (tanδ) due to the contribution of polar relaxation mechanisms and vacuole polarization, especially at low frequencies [٢٢]. With increasing frequency, the dielectric constant decreases because the dipoles are unable to keep up with rapid changes in the electric field, a behavior common in organic materials [٢٣]. The electrical conductivity of Schiff bases exhibits semiconducting behavior, dependent on a charge-jumping mechanism, where the alternating conductivity (σac) increases with increasing temperature and frequency. This is attributed to the presence of conjugated electronic systems that facilitate charge transfer across the molecular chain. This close relationship between chemical structure and electrical properties makes Schiff bases promising materials for applications in organic insulators, capacitors, and electronic sensors [٢٤, ٢٥]. Since most Schiff compounds are prepared as crystalline

powders or brittle materials, their electrical study in the solid state is limited due to the difficulty in molding and the uniformity of their electrodes. Therefore, incorporating Schiff compounds into an insulating polymer matrix such as polyvinyl alcohol, polyvinyl chloride, or polyacrylamide is a practical and efficient solution for preparing thin films suitable for electrical measurements. Polyvinyl alcohol is widely used because it is environmentally friendly, readily soluble, inexpensive, and can be easily molded. PVA acts as a mechanically supportive medium and a stable electrical insulator, while the Schiff compound retains its active centers responsible for polarization and charge transfer. This approach allows for the precise study of the dielectric constant, dielectric loss, and alternating current conductivity and is widely used in characterizing non-self-molding organic materials. Several studies have demonstrated that composite films of PVA and active organic compounds exhibit uniform and physically explainable electrical behavior[٢٦-٢٨] .

this study, a series of Schiff base compounds were prepared via condensation reactions between indole-٣-carboxaldehyde and various amines (٤-aminoacetophenone, ٢-aminobenzothiazole, ٢-aminothiazole, ٢-aminopyridine, and ٥-amino-١,٣,٤-thiadiazole-٢-thiol). Fourier transform infrared spectroscopy (FTIR) and proton nuclear magnetic resonance (^{1}H-NMR) were used to confirm the formation of the azimine bond (–C=N–) and the validity of the proposed structures. In the next step, films of these synthesized compounds with polyvinyl alcohol are prepared to measure their electrical properties.

٢. Experimental

٢.١. Chemicals and Instrumentations

All the chemicals and solvents were acquired directly from the companies Sigma-Aldrich, SDH, or Riedel-de haën and were used in their original form without undergoing any purification or alteration. To analyze the materials prepared, Infrared spectroscopy was conducted using a Shimadzu, Japanese company, The technique operates in the wave number range of (٤٠٠٠-٤٠٠) cm-١, in the laboratories of the College of Science, University of Diyala, Iraq. The structure of the prepared compounds was also diagnosed using nuclear magnetic resonance, using a Bruker type device, ٤٠٠ Hz, at the University of Tehran, Iran. At last, for studying dielectric properties, the GW INSTEK LCR-٨١٠٥G set with a frequency range from ١٠ kHz to ٥٠٠٠ kHz was utilized in the Department of Physics, College of Science, University of Diyala.

٢.٢. Synthesis of the Schiff Bases:

A ٠.٠١ M ethanolic solution of amines (٤-aminoacetophenone, ٢-aminobenzothiazole, ٢-aminothiazole, ٢-aminopyridine and ٥-amino-١,٣,٤-thiadiazole-٢-thiol) was added, with continuous stirring, to a ٠.٠١ M indole-٣-carboxaldehyde solution dissolved in ١٠ mL of ethanol. Three drops of glacial acetic acid were then added to the mixture, and refluxing was conducted for one hour. The mixture was then allowed to cool to room temperature, the solid was filtered, washed three times with ethanol (٥ mL), and then with diethyl ether (١٠ mL). It was dried at ٦٠°C for eight hours. The crude product was recrystallized with ethanol to obtain the corresponding Schiff base[٢٩]. Figure ١ shows a diagram illustrating the preparation of Schiff bases.

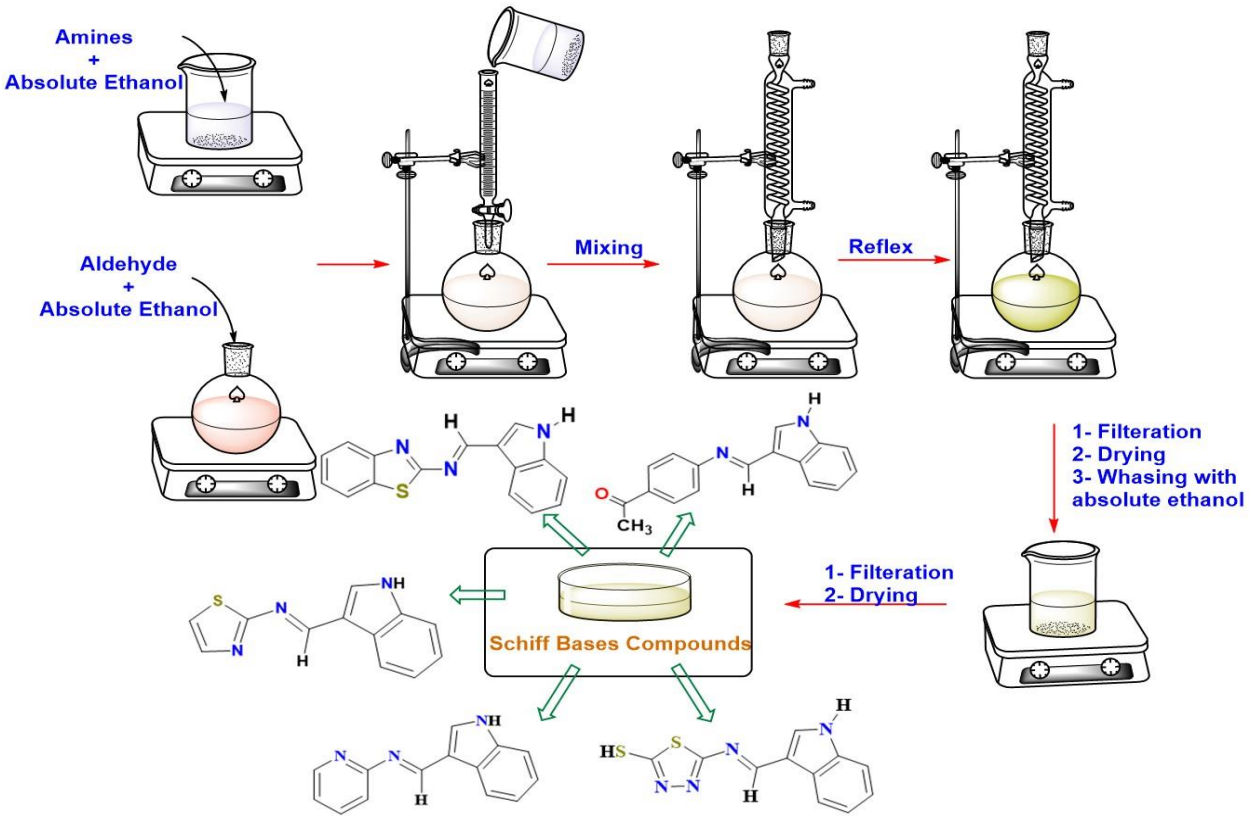

Figure (١): Schematic diagram illustrating the preparation of Schiff bases.

٢.٣.Preparation of Schiff Base/PVA Films:

Schiff base (M١-M٥)/ Polyvinyl alcohol (PVA) was prepared by dissolving ١ g of PVA in ٢٠ mL of warm distilled water, to which ٠.٠٥ g of Schiff base compounds (M١-M٥) were added separately. The mixture was vigorously mixed and heated to ٥٠°C for ١ hour to obtain a homogeneous solution. The solution was then sonicated for ١٥–٢٥ min at room temperature before being poured onto a glass plate and allowed to dry at room temperature. The prepared PVA-based Schiff base films were then removed and dried for electrical characterization.

٢.٤. Dielectric Constant Measurements:

To measure the dielectric properties of the prepared films, a ١ cm circle diameters was cut from film to appropriate the diameter of electrodes in (GW INSTEK LCR-٨١٠٥G) LCR meter. The real permittivity (real dielectric constant) (Ɛ'), imaginary permittivity (imaginary dielectric constant) (Ɛ''), loss factor (tan (δ) and current conductivity (σ_{ac}) were calculated according to the measured dielectric properties. Dielectric studies were conducted at various frequencies (١٠kHz -٢٠٠٠ kHz) at ٢٥ C°. The dielectric factors are defined by the complex permittivity (Ɛ*) in the equation[٣٠-٣٢]:

$$\varepsilon * = \varepsilon'(\omega) - \varepsilon''(\omega) \qquad (١)$$

Where: (Ɛ') is the real permittivity and (Ɛ'') is imaginary permittivity, (ω) represent the angular frequency; ($\omega = ٢\pi f$), while (f) is the applied frequency. Capacitance (C) was used to calculate the dielectric permittivity (Ɛ') using the next equation:

$$\varepsilon' = \frac{C\,d}{\varepsilon_o\,A} \qquad (٢)$$

Where: (d) is the thickness of film, (A) is the electrodes area, (ε_o) is free space permittivity will equal to = ٨.٨٥ ١٠$^{-١٢}$ F.m$^{-١}$ and (tan δ) is tangent delta:

$$\varepsilon''(\omega) = \varepsilon'(\omega)\,.\,tan\,\delta\,(\omega) \qquad (٣)$$

The alternating current conductivity (σ ac) can be determined by the subsequent equation:

$$\sigma = \varepsilon_o \varepsilon' \omega \tan\delta$$

٣. Results and Discussions:

٣.١. Synthesis of indole-٣-carbaldehyde Schiff base compounds:

Schiff bases were prepared by reacting indole-٣-carbaldehyde with various amines (٤-aminoacetophenone, ٢-aminobenzothiazole, ٢-aminothiazole, ٢-aminopyridine and ٥-amino-١,٣,٤-thiadiazole-٢-thiol) to form stable Schiff base compounds, as shown in Scheme (١).

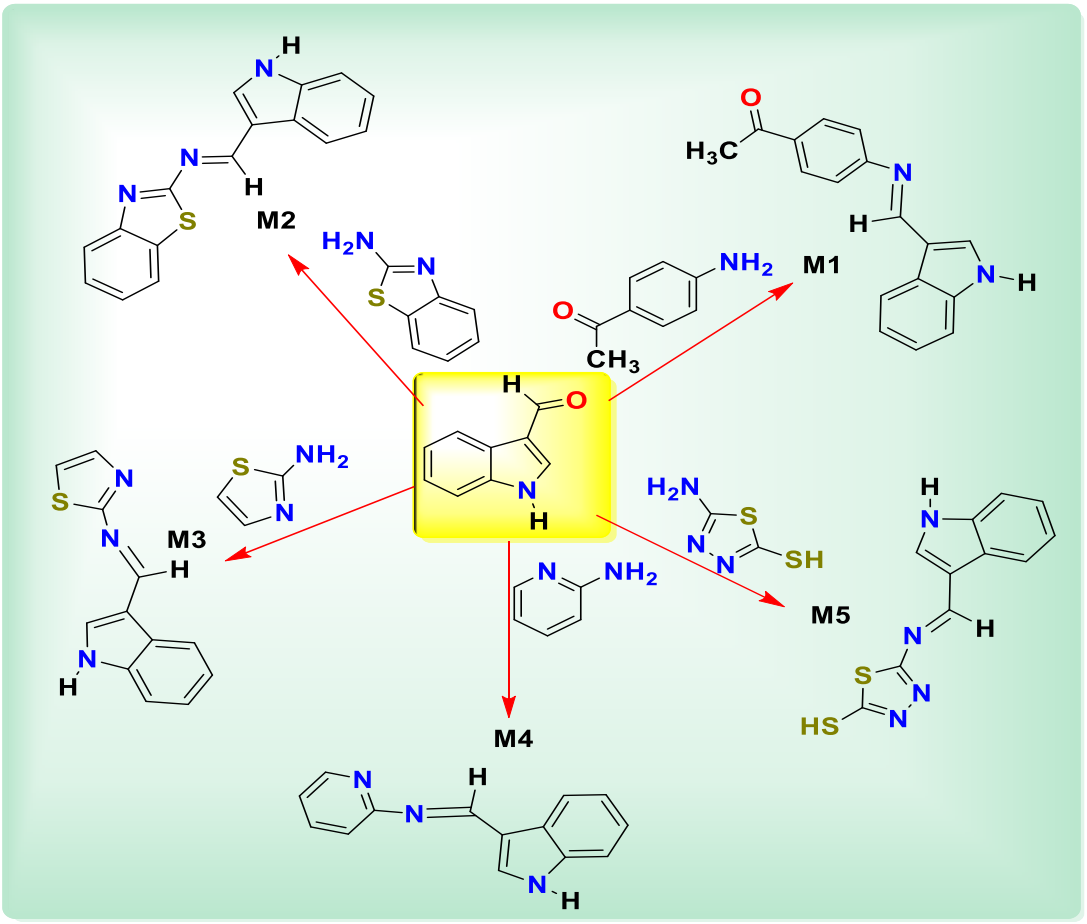

Scheme (١): Schiff bases prepared from indole-٣-carbaldehyde.

The mechanism for preparing Schiff bases between indole-٣-carbaldehyde and various amines in the acidic medium of glacial acetic acid follows the mechanism proposed in Scheme (٢) [١٨, ٣٣]

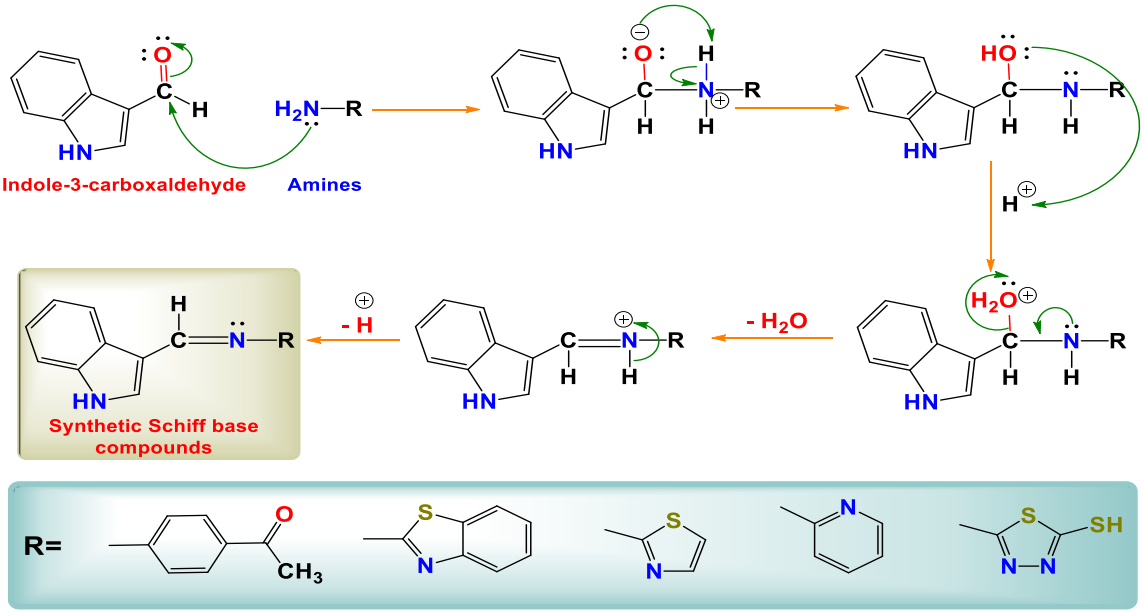

Scheme (٢): Proposed mechanism for preparing Schiff base compounds.

The physical properties of the synthesized compounds are listed in Table (١).

Table (١): The Physical properties of synthesized compounds.

No	Chemical Structure	Color	M. p (C^0)	M.Wt (g/mol)
١.	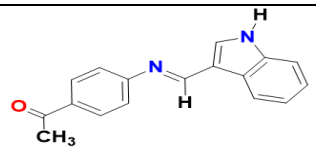	Yellow	٢٦٤-٢٦٦	٢٦٢
٢.	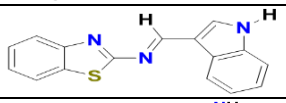	Yellow	٢٦٧-٢٦٩	٢٧٧
٣.	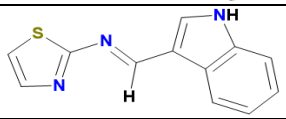	Brown	٢٠٢-٢٠٤	٢٢٧
٤.	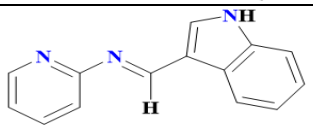	Pink	٢٠٠-٢٠٢	٢٢١
٥.	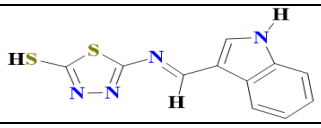	Dark Purple	٢٢٥-٢٢٧	٢٦٠

٣.٢. FTIR of Schiff base compounds:

٣.٢.١. FTIR of (E)-١-(٤-(((١H-indol-٣-yl) methylene) amino) phenyl) ethan-١-one (M١):

The infrared (FTIR) spectrum of the compound [(E)-١-(٤-(((١H-indol-٣-yl)methylene)amino)phenyl)ethan-١-one] in Figure (٢) shows a set of characteristic peaks that confirm the successful formation of a Schiff base while preserving the aromatic structures in the molecular composition. A strong band appears at ١٦٢٧ cm^{-1}, attributed to the stretching of the C=N bond of the imine, which is the main evidence for the formation of the Schiff base resulting from the condensation reaction between the amine group and the aldehyde. Meanwhile, the stretching band of the carbonyl C=O group of acetophenones is clearly observed at ١٧١٠ cm^{-1}. The characteristic N–H stretching range of the indole ring appears at ٣١٥٣ cm^{-1}, indicating that this ring remains unchanged during the reaction. Additionally, aromatic C–H stretching bands are recorded at ٣٠٤٧ cm^{-1}, and aliphatic C–H stretching bands in the range of ٢٨٢١–٢٩٧٨ cm^{-1} corresponding to the methyl group attached to the carbonyl. The vibrations of the aromatic C=C bonds appear near ١٥١٧ cm^{-1}, while the C–N stretching bands are observed at ١٢٤٠ cm^{-1}, which also supports the presence of the imine bond. Bending out-of-plane (=C–H) bands are also observed at ٧٥٢ cm^{-1}, which are characteristic of aromatic rings and the indole ring. In general, the distribution of these bands and their agreement with the expected values provide strong evidence of the successful synthesis of the target compound and the formation of the Schiff base while preserving the aromatic structures and the indole structure.

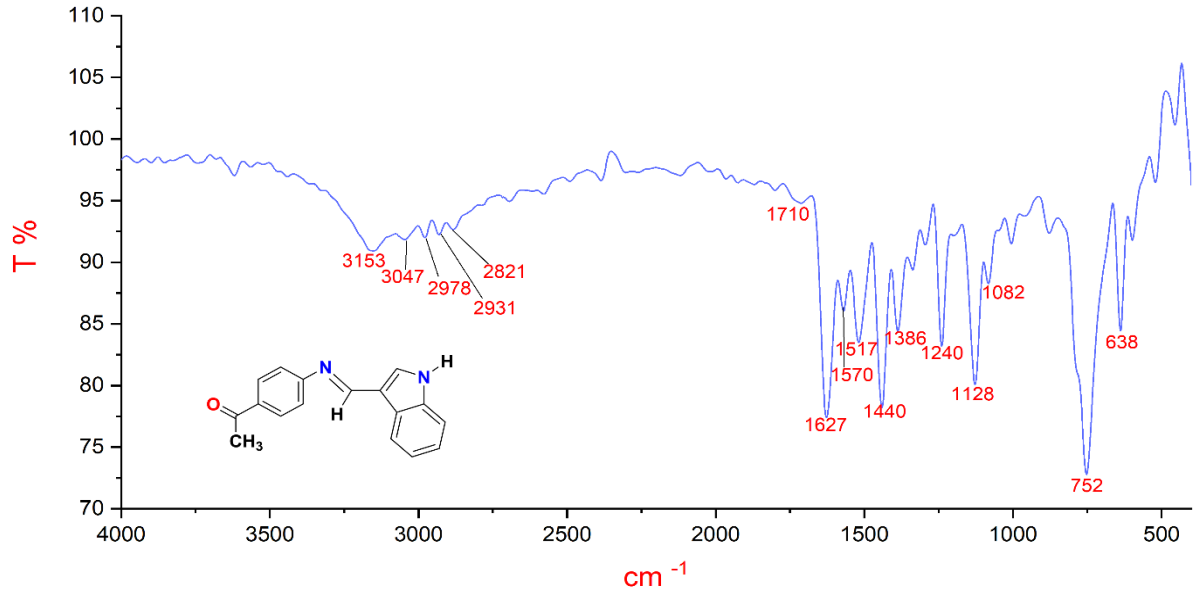

Figure (٢): FTIR of (E)-١-(٤-(((١H-indol-٣-yl) methylene) amino)phenyl)ethan-١-one.

٣.٢.٢. FTIR of [(E)-N-(benzo[d]thiazol-٢-yl)-١-(١H-indol-٣-yl) methanimine] (M٢):

The FTIR spectrum of the compound (E)-N-(benzo[d]thiazol-٢-yl)-١-(١H-indol-٣-yl)methanimine shows a range of spectral possibilities that confirm the formation of a Schiff base and the conservation of the indole and benzothiazole groups (Figure (٣)). The imine C=N extension is a prominent band typically seen at ١٥٩٧ cm^{-1}, indicating the formation of an azomethine bond following the reaction of the amine with the aldehyde. The N–H band of the indole ring is observed in the ٣١٣٦ cm^{-1} range, confirming the retention of the protonated nitrogen group. Furthermore, C=C aromatic ring vibrations appear around ١٤٦٩ cm^{-1}, aromatic C–H extension spectra at ٣٠٤٩ cm^{-1}, and C–N/imino spectra at ١٢٤٠ cm^{-1}. Additionally, out-of-plane bending (=C–H) at ٧٣٨ cm^{-1} provides a signature pattern for the rings

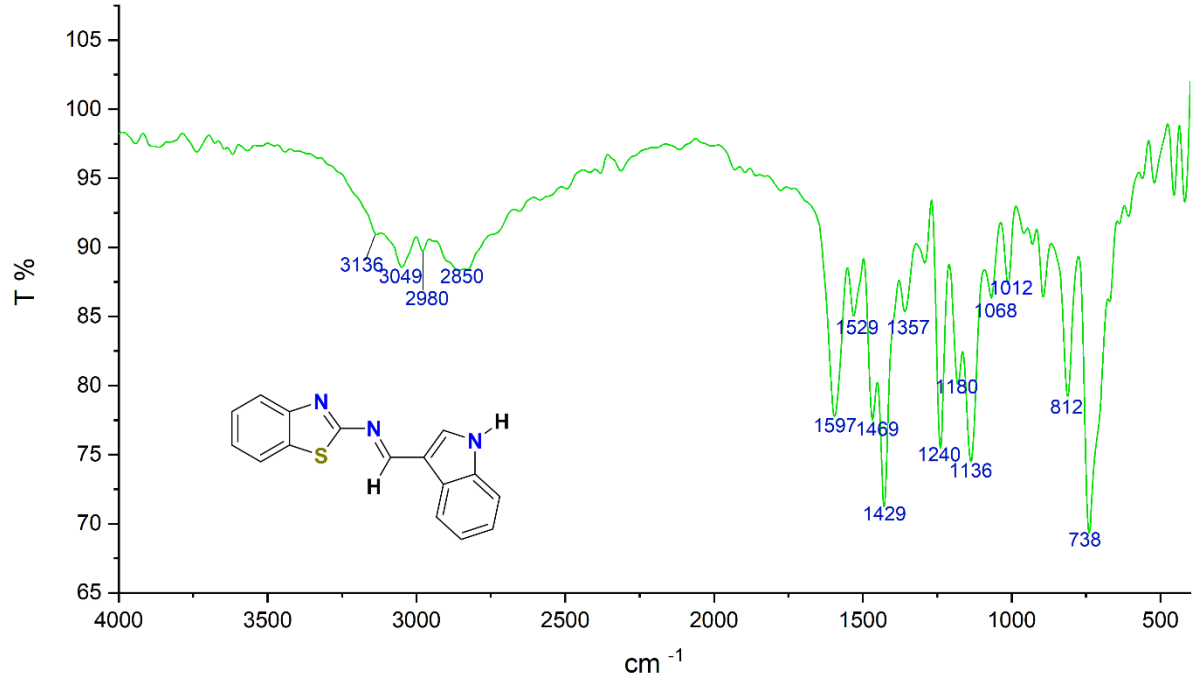

Figure (٣): FTIR of (E)-N-(benzo[d]thiazol-٢-yl)-١-(١H-indol-٣-yl)methanimine.

٣.٢.٣. FTIR of (E)-١-(١H-indol-٣-yl)-N-(thiazol-٢-yl)methanimine (M٣):

The infrared spectrum (FTIR) of the compound (E)-N-(benzo[d]thiazol-٢-yl)-١-(١H-indol-٣-yl)methanimine in Figure (٤) shows a strong band at around ١٦٣٣ cm^{-1} attributed to the stretching of the imine bond (C=N), confirming the formation of a Schiff base resulting from the reaction of the imine group in indole with the aldehyde group derived from benzothiazole. The N–H band of the indole ring is expected to appear around ٣١٦٩ cm^{-1}, indicating that the ring remains intact and has not undergone side reactions. The vibrations of the aromatic bonds (C=C) appear near ١٥١٤ cm^{-1}, while the aromatic C–H vibrations extend to about ٣٠٥٩ cm^{-1}, with the C–N band observed around ١٣٤٠ cm^{-1}. These bands collectively form a spectral fingerprint consistent with the proposed structure of the compound, confirming its inclusion of a Schiff base (C=N) while preserving the aromatic rings (indole, benzene, and thiazole) without decomposition or side reactions.

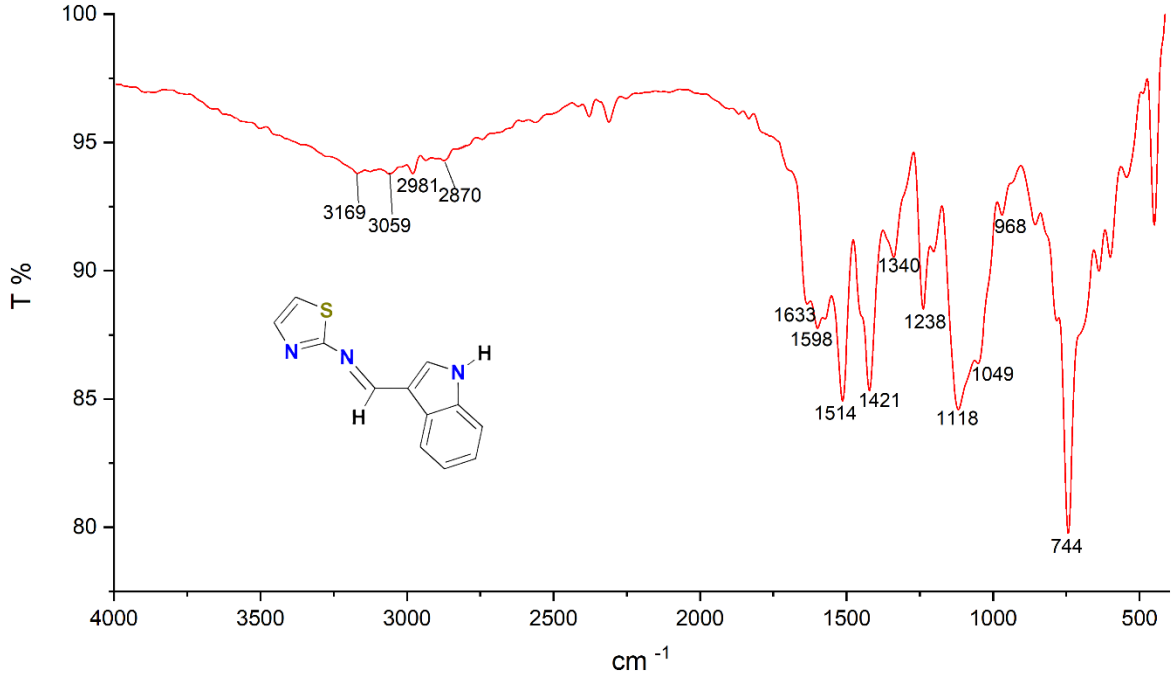

Figure (٤): FTIR of (E)-١-(١H-indol-٣-yl)-N-(thiazol-٢-yl)methanimine.

٣.٢.٤. FTIR of (E)-١-(١H-indol-٣-yl)-N-(pyridin-٢-yl)methanimine (M٤):

The FTIR spectrum shown in Figure (٥) for the compound (E)-١-(١H-indol-٣-yl)-N-(pyridin-٢-yl)methanimine exhibits a characteristic band for the imine bond (C=N) at ١٦٢٢ cm^{-1}, confirming the formation of a Schiff base resulting from the condensation reaction between the amine group in indole and the hydroxyl group derived from pyridine. The N–H range of the indole ring appears at ٣١٥٣ cm^{-1}, indicating the presence of the protonated nitrogen atom and the integrity of the indole ring structure. The vibrations of the aromatic rings (C=C) are observed at ١٤٣٦ cm^{-1}, in addition to the aromatic C–H range near ٣٠٤١ cm^{-1}. The expected C–N ranges are also recorded at ١٢٣٠ cm^{-1}, supporting the presence of the carbon-nitrogen bond, while out-of-plane =C–H vibrations appear at ٧٤٨ cm^{-1} as a distinctive signal for aromatic and pyridine structures. In general, the distribution of these bands corresponds to the spectral fingerprint of Schiff bases containing indole and pyridine, confirming the success of the

synthesis while maintaining the rings without structural degradation.

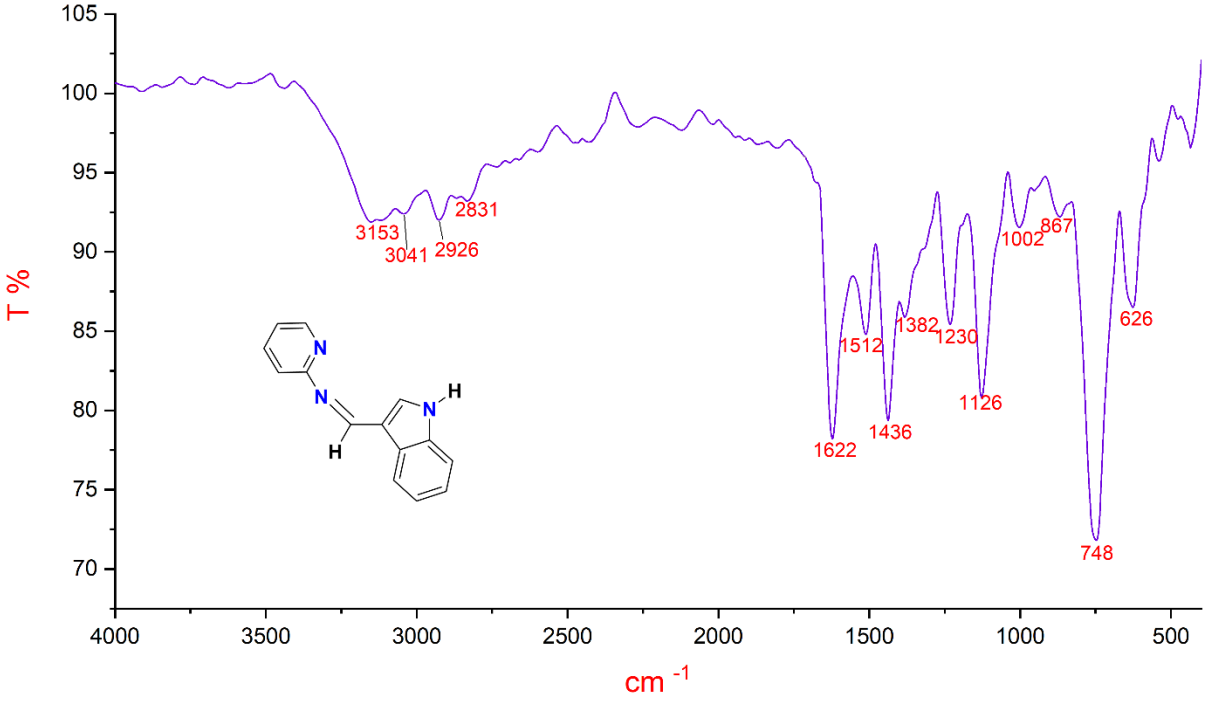

Figure (٥): FTIR of (E)-١-(١H-indol-٣-yl)-N-(pyridin-٢-yl)methanimine.

٣.٢.٥. FTIR of (E)-٥-(((١H-indol-٣-yl)methylene)amino)-١,٣,٤-thiadiazole-٢-thiol (M٥):

The Fourier transform infrared (FTIR) spectrum shown in Figure (٦) for the compound (E)-٥-(((١H-indol-٣-yl)methylene)amino)-١,٣,٤-thiadiazole-٢-thiol is expected to exhibit the characteristic features of Schiff base formation, in addition to the presence of indole and thiadiazol rings with the thiol group. A characteristic C=N imine bond band appears at ١٦١٦ cm^{-1}, confirming the formation of an azomethine bond resulting from the condensation reaction of the thiadiazol imine group with the indole aldehyde group. The N–H band of the indole ring appears at ٣١٥٧ cm^{-1}, indicating that the nitrogen atom remains in its protonated state. A weak and characteristic S–H band of the thiol group is likely to appear at ٢٥٧٨ cm^{-1}. The aromatic C=C vibrations are attributed to the band at ١٤٣٦ cm^{-1}. The aromatic C–H vibrations appear at ٣٠٤٥ cm^{-1}, and the C–N band at ١٢٣٤ cm^{-1} supports the presence of carbon-nitrogen bonds, while the off-plane bends of the =C–H bonds at ٧٤٦ cm^{-1} indicate the aromatic character of the rings. In general, the agreement of these bands with the expected values provides strong evidence for the successful preparation of a Schiff base between indole and thiadiazol with the compound retaining the thiol group, which contributes to its synergistic properties and its ability to chemisorption.

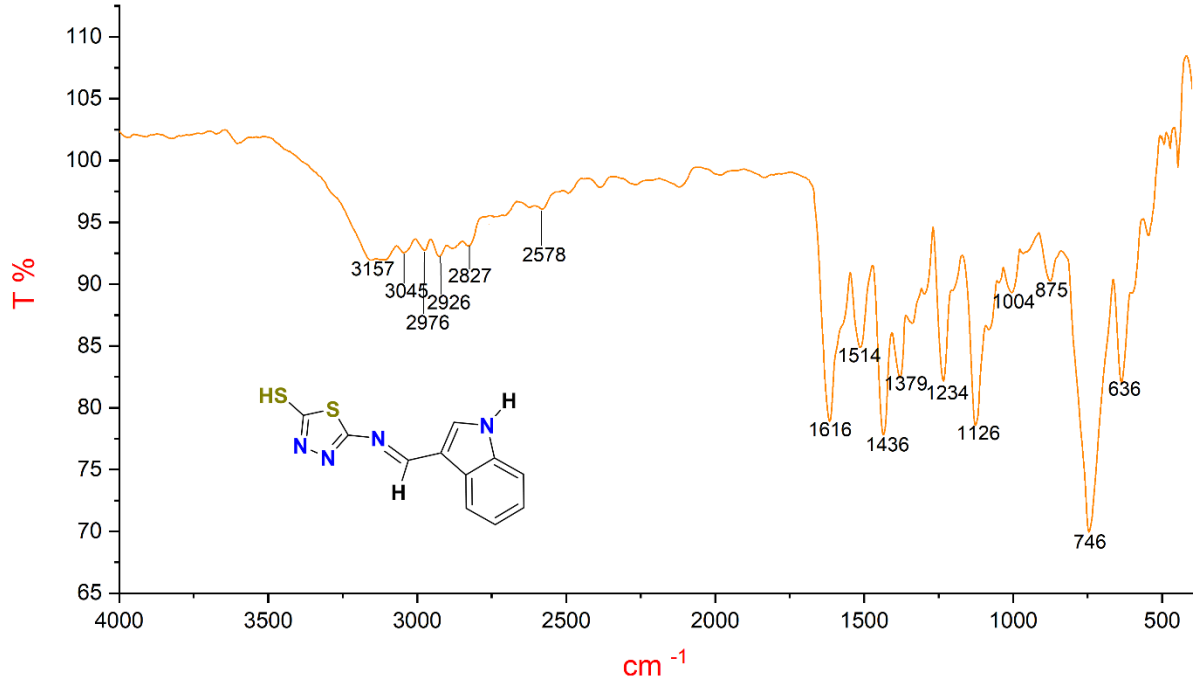

Figure (٦): FTIR of (E)-٥-(((١H-indol-٣-yl)methylene)amino)-١,٣,٤-thiadiazole-٢-thiol.

٣.٣. H-NMR of Schiff base compounds:

٣.٣.١. H-NMR of (E)-١-(٤-(((١H-indol-٣-yl) methylene) amino) phenyl) ethan-١-one (M١):

Figure (٧) shows the proton nuclear magnetic resonance spectrum of compound M١. The spectrum exhibits three singlet signals at ١٠.٨٥, ٩.٩٧, and ٧.٨٢ ppm, which are attributed to N-H, C-H (azomethen), and C-H٨ protons, respectively, with an integral corresponding to one proton. The presence of these signals is evidence of a successful reaction to form the desired product. The spectrum also shows a doublet signal at ٧.٥١ ppm and another at ٧.٣٧ ppm, with an integral corresponding to one proton, which are attributed to H٦ and H٣ protons. The doublet signals at ٧.٤٢٥ ppm and ٧.٢٧ ppm, with an integral corresponding to two protons, are attributed to H١٧, H١٥, and H١٤, H١٨ protons, respectively, with a J constant of ٧.٨٨ Hz. The spectrum also showed two triplet signals at ٧.٠٢ and ٦.٨٥, with an integral corresponding to a proton, attributed to C-H١,٢ protons, and a J constant of ٨ Hz. The aliphatic -CH_3 was found as a singlet signal at ٢.٤٨ ppm with integration of ٣ protons.

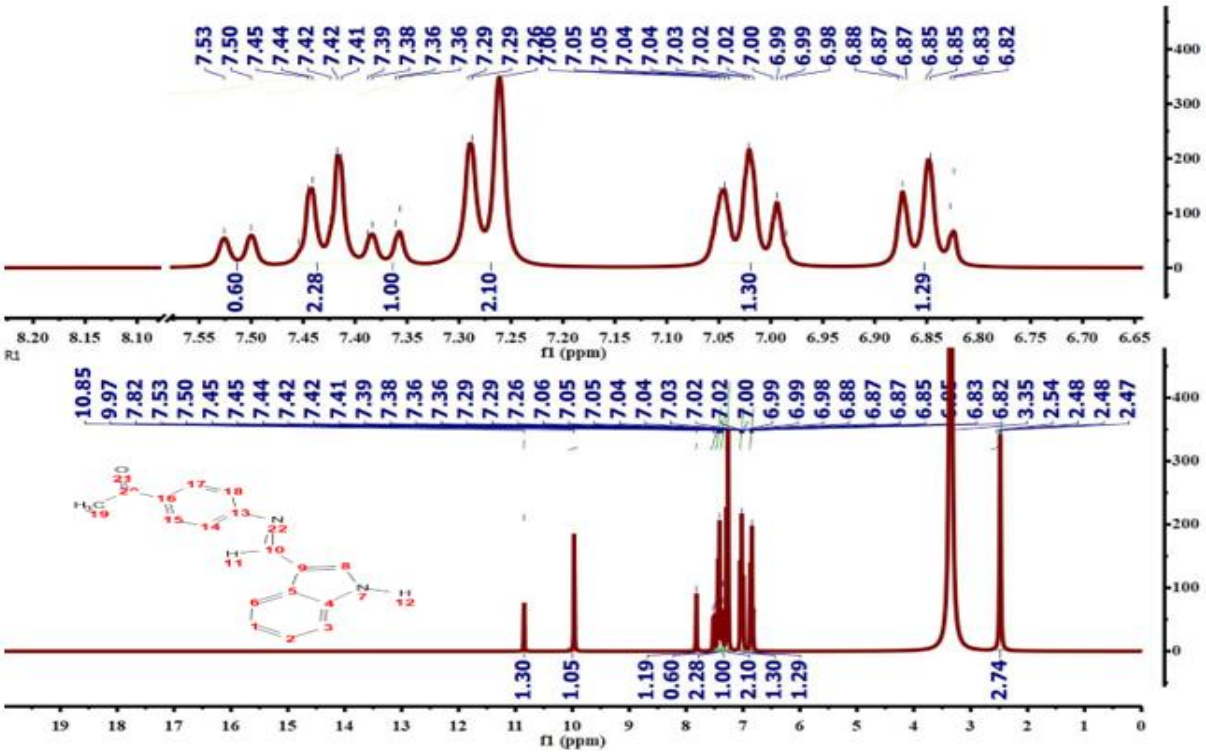

Figure (٧): H-NMR of (E)-٥-(((١H-indol-٣-yl)methylene)amino)-١,٣,٤-thiadiazole-٢-thiol.

٣.٣.٢. H-NMR of (E)-N-(benzo[d]thiazol-٢-yl)-١-(١H-indol-٣-yl)methanimine (M٢):

The proton nuclear magnetic resonance spectrum of compound M٢ in Figure (٨) showed three singlet signals at ١٠.٩٤, ١٠.١٦, and ٨.٤١ ppm, attributed to N-H, C-H (azomethen), and C-H٨ protons, respectively, with an integral corresponding to one proton .

The spectrum also showed four doublet signals at ٨.١٦, ٧.٨٥, ٧.٦١, and ٦.٨٩ ppm, with an integral corresponding to one proton and a coupling constant of ٧.٨٨–٨.٠٠ Hz. These doublet signals are attributed to H٣, H٦, H١٥, and H١٨ protons, respectively. Furthermore, the spectrum showed a triplet signal at ٧.٠٥ ppm which is attributed to the H١٤ proton with a coupling constant of ٨ Hz, while the multiple signals in the range of ٧.٣٧-٧.٢٥ ppm can be assigned to the H١٣, H١, H٢ protons. The spectrum shows the methoxy group protons as a singlet signal at ٢.٤٧ ppm and an integral corresponding to three protons.

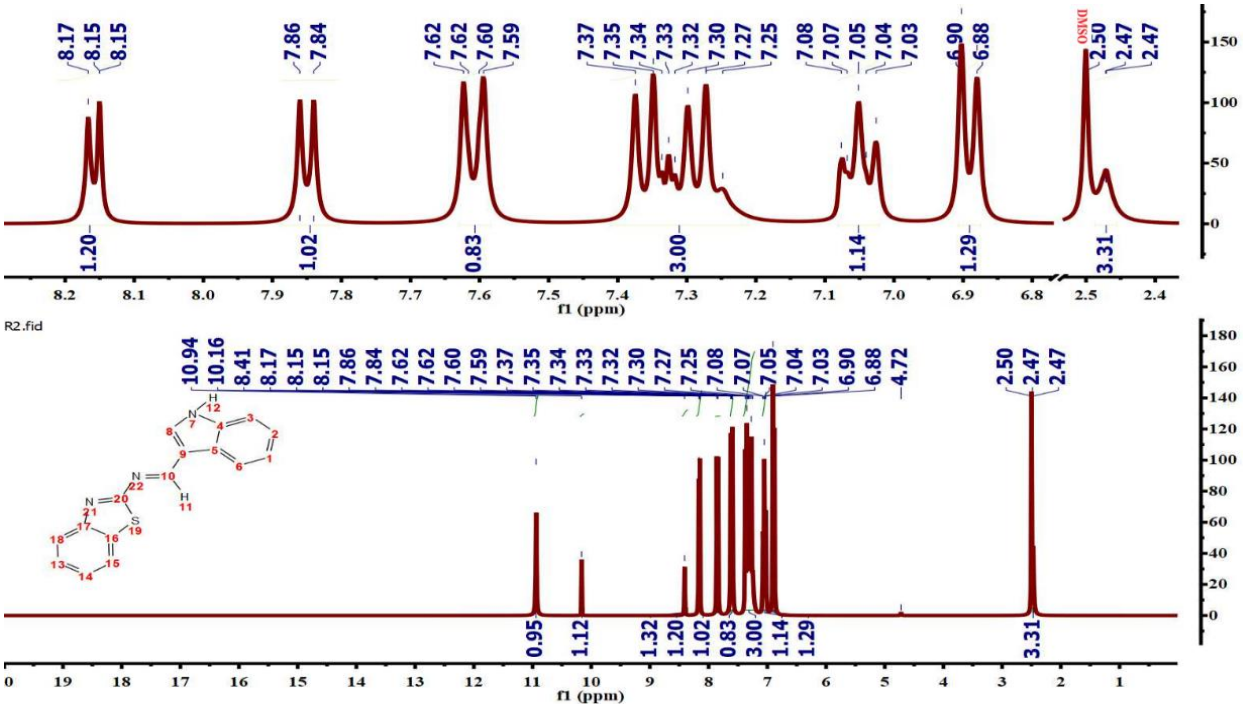

Figure (٨): H-NMR of (E)-N-(benzo[d]thiazol-٢-yl)-١-(١H-indol-٣-yl)methanimine.

٣.٣.٣. H-NMR of (E)-١-(١H-indol-٣-yl)-N-(thiazol-٢-yl)methanimine (M٣):

The proton nuclear magnetic resonance spectrum of compound M٣ in Figure (٩) showed three singlet signals at ١١.٠٧, ٨.٥٨, and ٧.٦٢ ppm, attributed to N-H, C-H (azomethen), and C-H٨ protons, respectively, with an integral corresponding to one proton .

Moreover, the spectrum showed four doublet signals at ٧.٥٣, ٧.٣٩, ٧.٢٦٥, and ٧.١٧٥ ppm, with an integral corresponding to one proton and a coupling constant of ٧.٨٨–٨.٠٠ Hz. These doublet signals are attributed to H٣, H٦, H١٣, and H١٤ protons, respectively. Furthermore, the spectrum showed two triplet signals at ٧.٠٦٥ and ٧.٩٧ ppm which are attributed to the H١ and H٢ protons with a coupling constant of ٨ Hz. The spectrum shows the methoxy group protons as a singlet signal at ٢.٣٤ ppm and an integral corresponding to three protons.

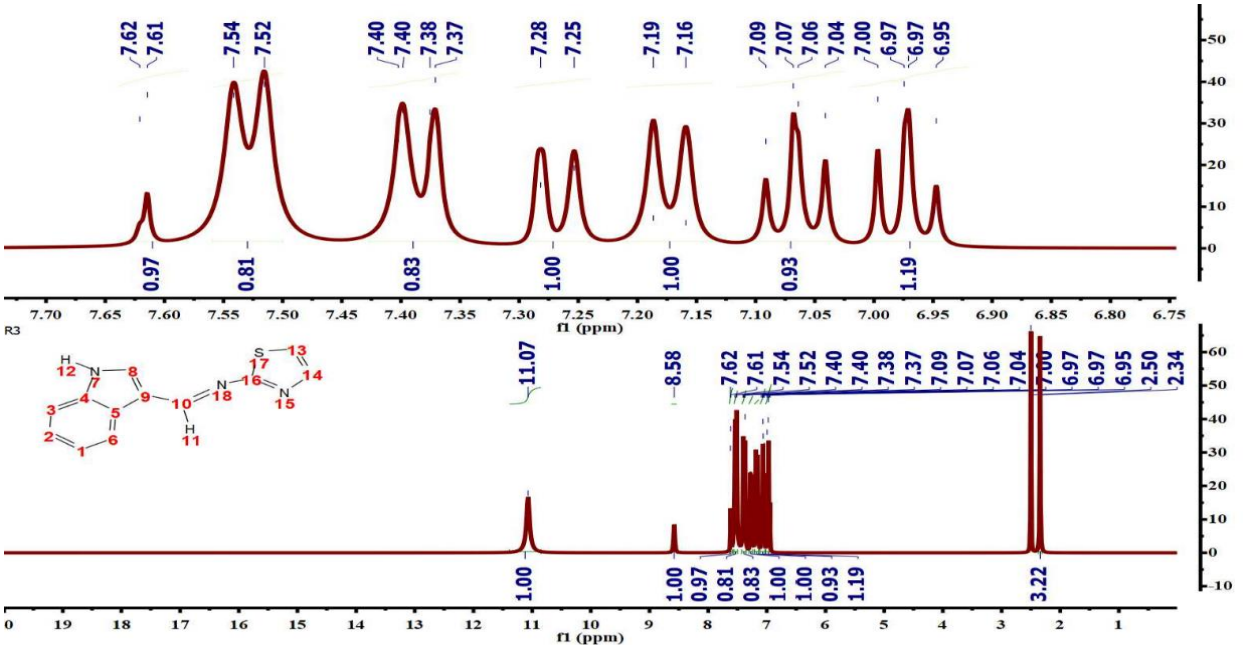

Figure (٩): H-NMR of (E)-١-(١H-indol-٣-yl)-N-(thiazol-٢-yl)methanimine.

٣.٣.٤. H-NMR of (E)-١-(١H-indol-٣-yl)-N-(pyridin-٢-yl)methanimine (M٤):

The proton nuclear magnetic resonance spectrum of compound M٤ in Figure (١٠) showed three singlet signals at ١٠.٩٣, ١٠.١٤, and ٨.٤١ ppm, attributed to N-H, C-H (azomethen), and C-H٨ protons, respectively, with an integral corresponding to one proton .

Furthermore, the spectrum showed three doublet signals at ٧.٥٩, ٧.٣٥٥ and ٧.٢٧٥ ppm, with an integral corresponding to one proton and a coupling constant of ٨.٠٠ Hz. These doublet signals are attributed to H١٤, H١٧ and H٣ protons, respectively. Furthermore, the spectrum showed a triplet signal at ٧.٠٣ ppm which is attributed to the H١٣ proton with a coupling constant of ٨.٠٠ Hz. The spectrum showed overlapping signals at ٦.٨٠-٦.٩٥ ppm with an integration corresponding to four protons of H١٨, H١, H٢, and H٦. The spectrum shows the methoxy group protons as a singlet signal at ٢.٠٣ ppm and an integral corresponding to three protons.

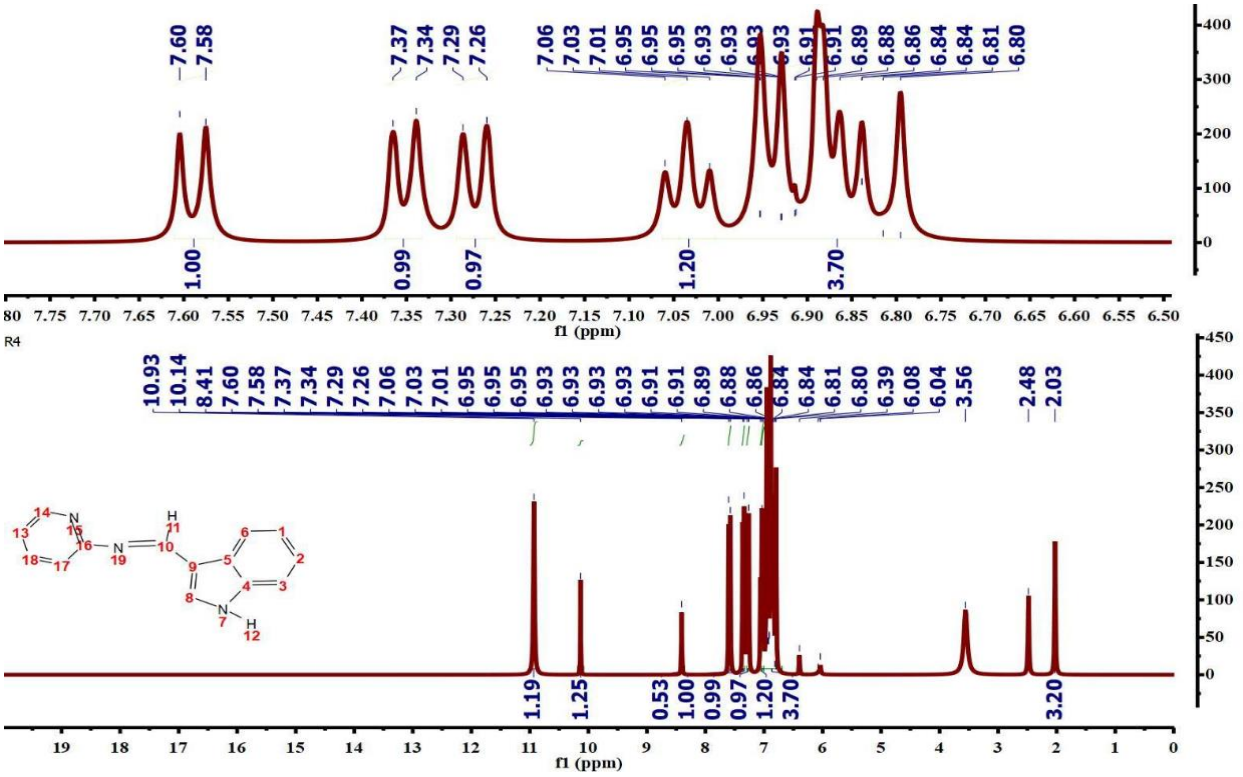

Figure (١٠): H-NMR of (E)-١-(١H-indol-٣-yl)-N-(pyridin-٢-yl)methanimine.

٣.٣.٥. H-NMR of (E)-٥-(((١H-indol-٣-yl)methylene)amino)-١,٣,٤-thiadiazole-٢-thiol (M٥):

The proton nuclear magnetic resonance spectrum of compound M٥ in Figure (١١) showed four singlet signals at ١١.٠٦, ٩.٩٢, ٨.١٧, and ٨.٠٤ ppm, attributed to N-H, S-H, C-H (azomethen), and C-H٨ protons, respectively, with an integral corresponding to one proton .

Moreover, the spectrum showed two doublet signals at ٧.٥٢, and ٧.٣٧ ppm, with an integral corresponding to one proton and a coupling constant of ٧.٨٦ Hz. These doublet signals are attributed to H٣ and H٦ protons, respectively. Furthermore, the spectrum showed two triplet signals at ٧.٠٦٥ and ٧.٩٧ ppm which are attributed to the H١ and H٢ protons with a coupling constant of ٧.٨٦ Hz. The spectrum shows the methoxy group protons as a singlet signal at ٢.٠٢ ppm and an integral corresponding to three protons.

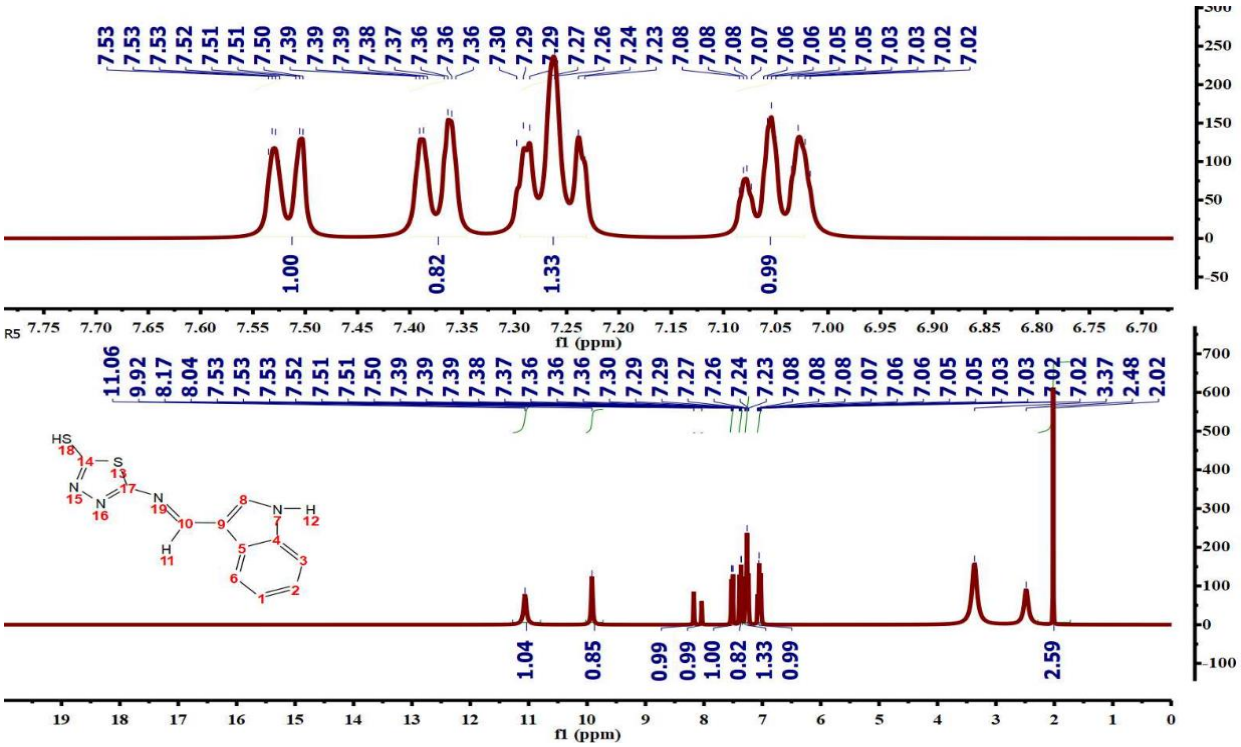

Figure (١١): H-NMR of (E)-٥-(((١H-indol-٣-yl)methylene)amino)-١,٣,٤-thiadiazole-٢-thiol.

٣.٤. Dielectric properties:

The real dielectric constant (permittivity) (Ɛ') data shown in Figure (١٢) for PVA films doped with various Schiff base compounds M١, M٢, M٣, M٤, and M٥ exhibit characteristic dielectric curves for polar polymers doped with active organic compounds. The Ɛ' decreases gradually with increasing frequency for all the compounds, but large discrepancies exist in their ε′ values. The Ɛ' is a characteristic of the storage of electrical energy in materials via various types of polarization, including directional polarization due to dipoles of -OH groups of PVA chains and polar groups such as C=N, N, S, O present in the Schiff base compounds. At low frequencies, the dipoles of the polymer matrix and the organic compounds can align in the direction of the applied electrical field; hence, Ɛ' is large for all the compounds. However, at high frequencies, the dipoles lose their ability to rotate rapidly in the direction of the applied field due to kinetic hindrance in the polymer matrix and the appearance of dielectric relaxation; hence, Ɛ' decreases with increasing frequency due to the reduction in directional polarization, leaving behind the time-faster electronic and ionic polarizations. The differences observed in the Ɛ' value for the membranes are due to the differences in the molecular structures of the Schiff bases, rather than the differences in the concentrations [٣٤]. The Ɛ' value for the compound M٤ is the highest for the entire frequency range. This is because the compound has a pyridine ring with a highly electronegative nitrogen atom, which increases the dipole moment and the asymmetry of the charges, thus increasing the directional polarization in the PVA membrane. The compound M٣, which has a thiazole ring, has the second-highest Ɛ' value, since the sulfur and nitrogen atoms increase the polarity of the compound. The compounds M١ and M٢ have moderate Ɛ' values because of the active polar groups, but the larger aromatic structure and the interaction with the PVA chains limit the free movement of the dipoles. The compound M٥ has low Ɛ' values because of the formation of strong hydrogen bonds between the thiol group, which is –SH, and the PVA chains, which limits the directional polarization and the ability to store electrical energy. This is further evidence that the real dielectric constant in these membranes is a

function mainly of the molecular structure and dipole moment of the introduced Schiff bases, and not their weight ratio, as postulated by the theoretical basis of the dielectric properties of polymer-organic systems [٣٥-٣٧].

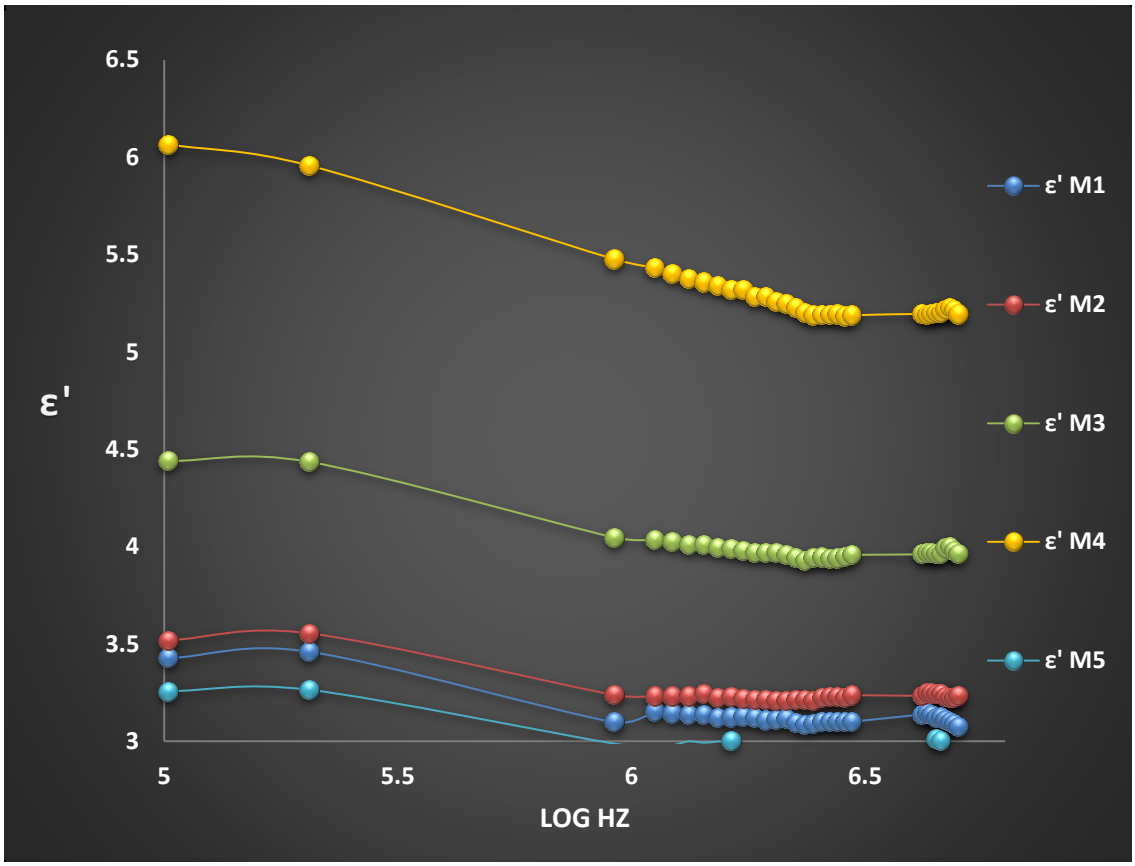

Figure (١٢): The real permittivity (Ɛ') of the synthesized Schiff base/PVA films.

The imaginary dielectric constant (permittivity) (Ɛ") curves for polyvinyl alcohol (PVA) films doped with varying Schiff bases M١-M٥ indicate a distinct rise with an increase in frequency for all the samples as shown in Figure (١٣). The Ɛ" values begin from a lower level at lower frequencies (log f ≈ ٥) and then rise steadily to attain their maximum at higher frequencies (log f ≈ ٦.٦-٦.٧). This is typical of polar polymers filled with active organic molecules, indicating the enhanced dielectric loss because of the lagging response of dipoles and charge flow compared to the alternating electric field. Ɛ" is the measure of the electrical energy lost in the material as heat, mainly because of the dielectric relaxation processes, localized charges, and dipole motion contributed by both the PVA chains and the polar groups in the Schiff bases. At lower frequencies, the dipole motion is in phase with the applied electric field, and hence the Ɛ" values are lower. As the frequency is raised, these dipoles, especially those trapped inside the polymer matrix, are unable to follow the fast-changing electric field, thereby creating a substantial phase difference between the applied electric field and the material response, which is directly proportional to the Ɛ" value [٣٨].

Comparison of the membranes has shown significant differences in the absolute value of Ɛ", which is due to the difference in the molecular structure of the Schiff bases. The membrane with compound M٤ has the maximum value of Ɛ" for the entire frequency range. This is because the compound contains a pyridine ring with a nitrogen atom, which has high electron density, thus increasing the asymmetry of the distribution of the electric field, which in turn increases the relaxation and the charge transfer effect in the PVA

membrane, thus increasing the dielectric loss. The compounds M٣ and M٥ have the next highest Ɛ", with compound M٣ containing a thiazole ring, while compound M٥ contains a ١,٣,٤-thiadiazol ring with a thiol group (-SH). Both compounds have sulfur and nitrogen atoms, which increase the local polarization effect. However, the possibility of the formation of hydrogen bonds between the compounds and the PVA chains, which limit the motion of the dipoles, results in the compounds having the lowest Ɛ" compared to compound M٤. Compounds M١ and M٢ have the least ε″, which is due to the larger aromatic ring in the compounds. Overall, this phenomenon further confirms that the imaginary dielectric constant ε″ for these films is related to the extent of polarization, as well as the nature of heteroatoms (N, S) and molecular flexibilities of the Schiff bases and their interactions with the -OH groups from PVA. In addition, it further confirms that increasing Ɛ" with frequency characterizes the transition from energy storage characteristics to dielectric loss characteristics, which is vital for assessing these membranes for energy storage devices, frequency insulators, and sensors [٣٤, ٣٩, ٤٠].

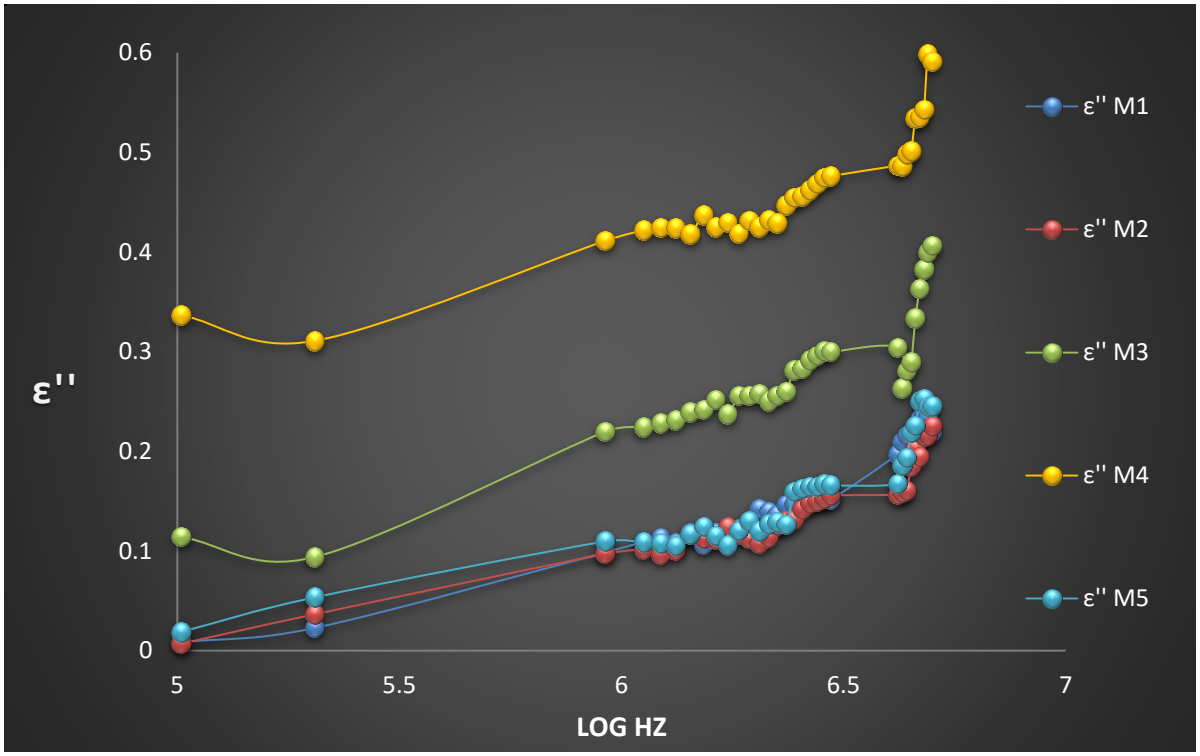

Figure (١٣): The imaginary permittivity (Ɛ") of the synthesized Schiff base/PVA films.

The alternating current conductivity (σ(ac)) values of polyvinyl alcohol (PVA) thin films doped with varying Schiff bases M١-M٥ indicate a consistent and pronounced rise with an increase in frequency for all samples, as observed in insulating-semiconducting polymer matrices doped with polar organic molecules Figure (١٤). At lower frequencies, σ(ac) indicates extremely low values ($١٠^{-٨}$-$١٠^{-٦}$ S/m), where charge carrier mobility is restricted due to their confinement within the energy wells of the polymer matrix, along with the predominance of localized hopping. With an increase in frequency, the excitation energy supplied to the system also increases, making it easier for charge transfer between the localized states in the energy gap. As a result, σ(ac) values increase with a power-law index ($\sigma(ac) \propto \omega^{s}$), signifying the predominance of frequency-dependent hopping[٣٤, ٤١]. The membranes display large differences in the absolute values of σ(ac), which depend solely on the structural differences of the Schiff bases and not on the concentration differences. The

membrane with compound M٤ displays the highest values of σ(ac) over the entire frequency range. This can be attributed to the presence of the electron-rich pyridine ring, which provides a higher density of local states and thus facilitates charge transfer in the PVA membrane. The compound M٣, with a thiazole ring, ranks closely after this compound, as the presence of sulfur and nitrogen helps facilitate electron hopping. The compounds M١ and M٢ have intermediate values, as these compounds have a balanced effect of polarity and structural restrictions in the polymer matrix. In contrast, compound M٥ displays lower values of σ(ac) at lower frequencies. The strong hydrogen bonds formed between the -SH group and the PVA chains are responsible for this effect, as they restrict charge transport. The effect of higher frequencies, however, overcomes this restriction, resulting in increased conductivity at higher frequencies. Thus, it can be concluded that the alternating conductivity of these polymer-organic compound membranes is due to the electron-hopping and polymer-organic interaction mechanisms, and that the molecular structure of Schiff bases plays a crucial role in determining the efficiency of electrical transport, thus making these compounds promising candidates for sensor, semiconductor membrane, and frequency-dependent insulating material applications [٢١, ٣٤, ٤٢, ٤٣].

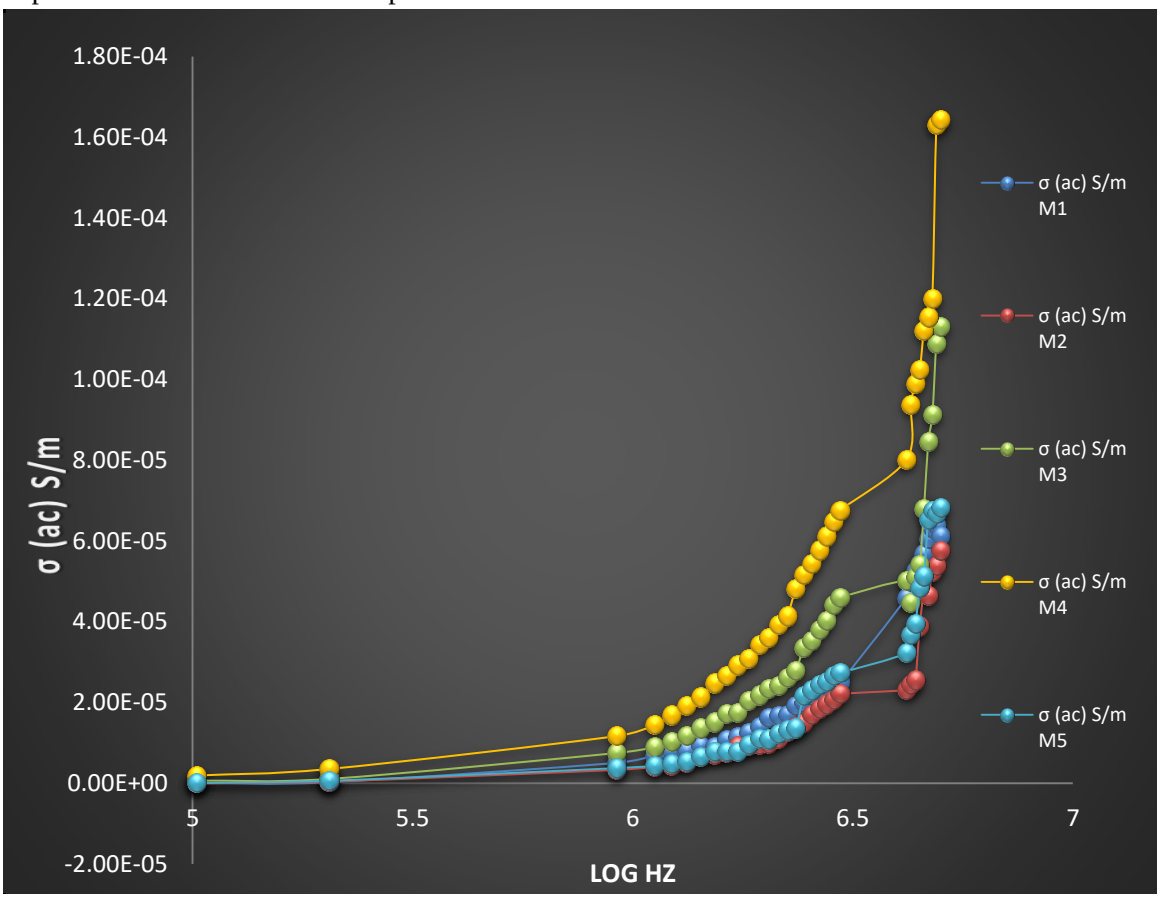

Figure (١٤): The conductivity (σ ac) of the of the synthesized Schiff base/PVA films.

Conclusion:

The study was able to show that M١-M٥ organic Schiff base compounds were successfully synthesized with high purity levels, as demonstrated through the measurement studies conducted. In addition to that, M١-M٥ organic Schiff base compounds were successfully incorporated into a polyvinyl alcohol membrane matrix, leading to highly enhanced previously studied properties of polyvinyl alcohol materials, thus proving the theory of the molecular structure of

organic compounds being a key component of matter. All membranes showed a decrease in the true dielectric constants with increasing frequencies; this is because of the limited dipole responses to high-frequency energies. However, the imaginary permittivity and alternating conductivity increased with the increasing frequencies because of the activated jump-type CT processes of the polymer membranes. The membrane that carried M٤ showed the maximum value of ε′, ε″, and σ(ac); this is because of the increased polarity level of the compound, which was a result of having a nitrogen-containing pyridine ring. However, M١ and M٢ showed reduced levels of ε″ and σ(ac); thus, they were the most stable membranes for electrical purposes. Based on the studies conducted, these materials can be directed to improved uses depending on the requirements of the compounds.

References:

[١] M. Andruh, "The exceptionally rich coordination chemistry generated by Schiff-base ligands derived from o-vanillin," *Dalton Transactions*, vol. ٤٤, no. ٣٨, pp. ١٦٦٣٣-١٦٦٥٣, ٢٠١٥.

[٢] L. A. Mohammed *et al.*, "A review on benzimidazole heterocyclic compounds: synthesis and their medicinal activity applications," *SynOpen*, vol. ٧, no. ٠٤, pp. ٦٥٢-٦٧٣, ٢٠٢٣.

[٣] D. R. Klein and L. S. Starkey, *Organic chemistry*. John Wiley & Sons, ٢٠٢٥.

[٤] L. A. Adnan, N. F. Alheety, A. H. Majeed, M. A. Alheety, and H. Akbaş, "Novel organic-inorganic nanohybrids (MnO٢ and Ag nanoparticles functionalized ٥-methoxy-٢-mercaptobenzimidazole): one step synthesis and characterization," *Materials Today: Proceedings*, vol. ٤٢, pp. ٢٧٠٠-٢٧٠٥, ٢٠٢١.

[٥] N. F. Alheety, A. H. Majeed, and M. A. Alheety, "Silver nanoparticles anchored ٥-methoxy benzimidazol thiomethanol (MBITM): Modulate, characterization and comparative studies on MBITM and Ag-MBITM antibacterial activities," in *Journal of Physics: Conference Series*, ٢٠١٩, vol. ١٢٩٤, no. ٥, p. ٠٥٢٠٢٦: IOP Publishing.

[٦] L. A. Mohammed, O. A. Nief, F. W. Askar, and A. H. Majeed, "Synthesis, characterization and antimicrobial activities of silver nanoparticles coated [١, ٣] thiazin-٤-one derivatives," in *Journal of Physics: Conference Series*, ٢٠١٩, vol. ١٢٩٤, no. ٥, p. ٠٥٢٠٢٨: IOP Publishing.

[٧] E. H. Anouar *et al.*, "Antioxidant properties of phenolic Schiff bases: structure–activity relationship and mechanism of action," *Journal of computer-aided molecular design*, vol. ٢٧, no. ١١, pp. ٩٥١-٩٦٤, ٢٠١٣.

[٨] S. Kataria *et al.*, "Design, synthesis, and computational analysis of oxazine-based Schiff bases as prospective analgesic and anti-inflammatory agents," *Journal of Molecular Structure*, p. ١٤٣٥٦٦, ٢٠٢٥.

[٩] M. Tyagi and M. Dubey, "A fight against cancer with advancement of Schiff base metal complexes: Future prospects," *Oral Oncology Reports*, vol. ١٣, p. ١٠٠٦٩٢, ٢٠٢٥.

[١٠] K. El-Baradie, Y. S. El-Sayed, N. El-Wakiel, B. M. Salem, and A. El-Nagar, "Novel indazole Schiff base metal chelates as potential antifungal agents: synthesis, characterization, and computational analysis," *Chemical and Biological Technologies in Agriculture*, vol. ١٢, no. ١, p. ٥٨, ٢٠٢٥.

[١١] M. Taha *et al.*, "Synthesis of ٢-methoxybenzoylhydrazone and evaluation of their antileishmanial activity," *Bioorganic & Medicinal Chemistry Letters*, vol. ٢٣, no. ١١, pp. ٣٤٦٣-٣٤٦٦, ٢٠١٣.

[١٢] A. C. Okechukwu, S. U. Omoraka, S. Bello, R. Amaeze, O. Joseph, and E. Okoro, "Schiff Bases and their Ability to Remove Heavy Metals," *IOSR Journal of Applied Chemistry*, vol. ١٥, no. ٧, pp. ٧-١٤, ٢٠٢٢.

[١٣] N. I. Normi, A. S. Abdulhameed, S. Surip, Z. A. ALOthman, L. D. Wilson, and A. H. Jawad, "Benzil Schiff base side-chain polymer-crosslinked chitosan via hydrothermal process for Reactive orange ١٦ dye removal: An optimized and comparative study with chitosan," *Journal of Polymers and the Environment*, vol. ٣١, no. ٥, pp. ١٩٨٦-٢٠٠٤, ٢٠٢٣.

[١٤] X. Zhong, Z. Li, R. Shi, L. Yan, Y. Zhu, and H. Li, "Schiff base-modified nanomaterials for ion detection: a review," *ACS Applied Nano Materials*, vol. ٥, no. ١٠, pp. ١٣٩٩٨-١٤٠٢٠, ٢٠٢٢.

[١٥] J. S. Aulakh, V. Kumar, and K.-H. Kim, "A review of the applications of Schiff bases as optical chemical sensors," *Trends in Analytical Chemistry*, vol. ١١٦, pp. ٧٤-٩١, ٢٠١٩.

[١٦] E. S. Gad, M. A. Abbas, M. A. Bedair, O. E. El-Azabawy, and S. M. Mukhtar, "Synthesis and applications of novel Schiff base derivatives as corrosion inhibitors and additives for improvement of reinforced concrete," *Scientific Reports*, vol. ١٣, no. ١, p. ١٥٠٩١, ٢٠٢٣.

[١٧] Y. Guo *et al.*, "Preparation and characterization of Schiff base metal complexes for high performance supercapattery," *Journal of Energy Storage*, vol. ٤٨, p. ١٠٣٩٥٦, ٢٠٢٢.

[١٨] E. Troschke, M. Oschatz, and I. K. Ilic, "Schiff-bases for sustainable battery and supercapacitor electrodes," in *Exploration*, ٢٠٢١, vol. ١, no. ٣, p. ٢٠٢١٠١٢٨: Wiley Online Library.

[١٩] S. M. Gomha, H. A. Ahmed, M. Shaban, T. Z. Abolibda, M. S. Khushaim, and K. A. Alharbi, "Synthesis, optical characterizations and solar energy applications of new Schiff base materials," *Materials*, vol. ١٤, no. ١٣, p. ٣٧١٨, ٢٠٢١.

[٢٠] Y. Wu, H. Lin, Y. Hu, F. Cai, and X. Zhang, "Electrical and degradation properties of epoxy insulating materials based on schiff bases," *ACS Applied Polymer Materials*, vol. ٦, no. ٢, pp. ١١٨٢-١١٩٠, ٢٠٢٤.

[٢١] A. R. Yaul, V. V. Dhande, G. B. Pethe, and A. S. Aswar, "Synthesis, characterization, biological and electrical conductivity studies of some Schiff base metal complexes," *Bulletin of the Chemical Society of Ethiopia*, vol. ٢٨, no. ٢, pp. ٢٥٥-٢٦٤, ٢٠١٤.

[٢٢] J. Wiley, "Impedance Spectroscopy Theory, Experiment, and Applications," ed, ٢٠٠٥.

[٢٣] A. Solmaz, İ. Kaya, and E. Bayır, "High thermal stability and dielectric performance of phenylhydrazine-based Schiff base oligomers obtained via oxidative polycondensation," *Journal of Materials Science: Materials in Electronics*, vol. ٣٦, no. ٣٦, p. ٢٢٨٥, ٢٠٢٥.

[٢٤] M. M. Aran and S. H. Abdulrahman, "Electrical conductance study of Schiff base in different solvents and temperatures: DFT calculation," *Bulletin of the Chemical Society of Ethiopia*, vol. ٣٩, no. ١, pp. ١٧٧-١٨٧, ٢٠٢٥.

[٢٥] S. M. Morgan, A. El-Sonbati, N. El-Ghamaz, S. Nozha, M. Diab, and M. El-Mogazy, "Characterization, geometrical structural, optical properties and electrical conductivity, and effect of type of derivatives of azo Schiff base quinoline on the optical energies gap and theoretical parameters," *Journal of the Indian Chemical Society*, p. ١٠٢٤٥٩, ٢٠٢٦.

[٢٦] J. Li, L. Qi, and H. Li, "Facile strategy to prepare light-weight PVA membrane based on schiff base

derivatives and MWCNTs for electromagnetic wave absorption," *The Journal of Physical Chemistry C*, vol. ١٢٠, no. ٤٠, pp. ٢٢٨٦٥-٢٢٨٧٢, ٢٠١٦.

[٢٧] B. F. Abdallaha, M. A. Younus, and I. J. Ibraheem, "Preparation, Characterization, Antimicrobial and Antitumor Activity of Chitosan Schiff base/PVA/PVP Au, Ag Nanocomposite in Treatment of Breast Cancer Cell Line," *Nanomedicine Research Journal*, vol. ٦, no. ٤, pp. ٣٦٩-٣٨٤, ٢٠٢١.

[٢٨] F. J. Moaen, T. A. Saleh, B. E. Jasem, A. A. Husain, and A. H. Oraibi, "Enhanced optical and dielectric properties of PVC films via plasma-treated Schiff base-modified metal oxide nanocomposites," *Journal of Materials Science: Materials in Electronics*, vol. ٣٦, no. ٢٨, p. ١٨١٤, ٢٠٢٥.

[٢٩] D. Sinha *et al.*, "Synthesis, characterization and biological activity of Schiff base analogues of indole-٣-carboxaldehyde," *European journal of medicinal chemistry*, vol. ٤٣, no. ١, pp. ١٦٠-١٦٥, ٢٠٠٨.

[٣٠] I. A. Latif, H. M. Abdullah, and M. H. Saleem, "Electrical and swelling study of different prepared hydrogel," *Am J Polym Sci*, vol. ٦, no. ٢, pp. ٥٠-٥٧, ٢٠١٦.

[٣١] I. Latif, E. E. AL-Abodi, D. H. Badri, and J. Al Khafagi, "Preparation, characterization and electrical study of (carboxymethylated polyvinyl alcohol/ZnO) nanocomposites," *American Journal of Polymer Science*, vol. ٢, no. ٦, pp. ١٣٥-١٤٠, ٢٠١٢.

[٣٢] I. Latif, T. B. Alwan, and A. H. Al-Dujaili, "Low frequency dielectric study of PAPA-PVA-GR nanocomposites," *Nanoscience and Nanotechnology*, vol. ٢, no. ٦, pp. ١٩٠-٢٠٠, ٢٠١٢.

[٣٣] E. Guliani, S. Banga, and V. V. Pathak, "Physicochemical Characterization of One-Pot Synthesized ٢-[(E)-(٤-Hydroxyphenylimino) methyl] phenol Schiff Base Using Orange Juice as Citrus-Derived Acidic Medium," *Waste and Biomass Valorization*, vol. ١٦, no. ١٠, pp. ٥٣٣٣-٥٣٤٣, ٢٠٢٥.

[٣٤] A. H. Majeed, E. T. B. Al-Tikrity, and D. H. Hussain, "Dielectric properties of synthesized ternary hybrid nanocomposite embedded in poly (vinyl alcohol) matrix films," *Polymers and Polymer Composites*, vol. ٢٩, no. ٧, pp. ١٠٨٩-١١٠٠, ٢٠٢١.

[٣٥] I. Popov, S. Cheng, and A. P. Sokolov, "Broadband dielectric spectroscopy and its application in polymeric materials," *Macromolecular Engineering: From Precise Synthesis to Macroscopic Materials and Applications*, pp. ١-٣٩, ٢٠٢٢.

[٣٦] H. G. El Gohary, T. F. Qahtan, H. G. Alharbi, G. Asnag, and A. Waly, "Studies of the structural, optical, thermal, electrical and dielectric properties of a polyvinyl alcohol/sodium alginate blend doped with Cu nanoparticles and ZnO nanorods as hybrid nanofillers for use in energy storage devices," *Journal of Polymers and the Environment*, vol. ٣١, no. ٧, pp. ٢٩٣٠-٢٩٤٠, ٢٠٢٣.

[٣٧] H. A. Badran and H. A. Hasan, "Dielectric constant and conductivity anisotropy measurements of Schiff base liquid crystal," in *Journal of Physics: Conference Series*, ٢٠٢١, vol. ١٩٩٩, no. ١, p. ٠١٢٠٤٤: IOP Publishing.

[٣٨] Q. Wang *et al.*, "Contributing factors of dielectric properties for polymer matrix composites," *Polymers*, vol. ١٥, no. ٣, p. ٥٩٠, ٢٠٢٣.

[٣٩] S. Patari and A. Nath, "Studies of temperature and frequency dependence of dielectric permittivities

of two Schiff's base liquid crystal compounds," *Journal of Molecular Liquids*, vol. ٢٣٠, pp. ٢٤٧-٢٥٣, ٢٠١٧.

[٤٠] H. Hassib and A. A. Razik, "Dielectric properties and AC conduction mechanism for ٥, ٧-dihydroxy-٦-formyl-٢-methylbenzo-pyran-٤-one bis-schiff base," *Solid state communications*, vol. ١٤٧, no. ٩-١٠, pp. ٣٤٥-٣٤٩, ٢٠٠٨.

[٤١] Z. H. Mahmoud, R. A. Al-Bayati, and A. A. Khadom, "In situ polymerization of polyaniline/samarium oxide-anatase titanium dioxide (PANI/Sm٢O٣-TiO٢) nanocomposite: structure, thermal and dielectric constant supercapacitor application study," *Journal of Oleo Science*, vol. ٧١, no. ٢, pp. ٣١١-٣١٩, ٢٠٢٢.

[٤٢] A. H. Majeed, W. A. Hussen, A. N. Abd, Z. H. Mahmoud, and E. Kianfar, "Graphene-tungsten oxide hybrid nanocomposites for high-performance dielectric films in conductive polymer matrices," *South African Journal of Chemical Engineering*, vol. ٥٣, no. ١, pp. ٣٠٣-٣١٨, ٢٠٢٥.

[٤٣] L. A. Mohammed *et al.*, "Design and characterization of novel ternary nanocomposite (rGO-MnO٢-PoPDA) product and screening its dielectric properties," *International Journal on Interactive Design and Manufacturing (IJIDeM)*, vol. ١٧, no. ٥, pp. ٢٣٨٧-٢٤٠١, ٢٠٢٣.